

4-Arylmethylisoxazol-5-one Derivatives – Novel Synthesis, Structural Studies, and Supramolecular Self-Assembly through Resonance-Assisted Hydrogen Bonding

Giovanni Grassi,^{*,[a]} Giuseppe Bruno,^[b] Francesco Risitano,^[a] Francesco Foti,^[a] Francesco Caruso,^[a] and Francesco Nicolò^[b]

Keywords: Ab initio calculations / Crystal structures / Density functional calculations / Reductions / Tautomerism

Arylmethylisoxazol-5-ones (**3**) were prepared by a new mild reductive procedure using tertiary amines containing a flexible N–CH–CH grouping. A concurrent process competed with the reduction, yielding fair quantities of chain-elongation products (**4**). The X-ray structures of two selected arylmethyl derivatives are reported and are shown to have the

expected different tautomeric arrangements. The unusual features of the NH-tautomer (**3e**) were interpreted in terms of the RAHB (resonance-assisted hydrogen bond) model and its relative stability was investigated by ab initio and DFT calculations.

Introduction

The hydrogen bond continues to excite a great deal of interest because of the role it plays in processes such as the stabilization of crystal architectures,^[1] the loss of information in DNA^[2] or even the construction of chemical memory devices.^[3]

Particular attention has been focussed on heteroconjugated systems in which an inter- or intramolecular hydrogen bond may be strengthened through strict correlation with a conjugated π -bond in the heterosystem. This phenomenon, called Resonance-assisted Hydrogen Bonding (RAHB), has been interpreted on the basis of a synergistic interplay between π -system delocalization and hydrogen bond formation.^[4] In this context, a variety of heteroconjugated systems have been studied with the aim of determining crystal engineering rules for the production of materials with potential practical applications.^[5]

In the light of studies carried out into the chemistry of heterocycles, we turned our attention to those heteroaromatic cyclic systems in which proton migration along a hydrogen bond may be accompanied by tautomeric changes and possibly also a consequent RAHB effect with supramolecular autoassembly processes.

Our research group has recently investigated 4-(arylmethyl)isoxazol-5-one derivatives, defining a synthetic approach and determining their tautomeric compositions in solution.^[6] The structures of these compounds, which can exist in the four forms depicted in Figure 1, seemed particu-

larly suitable for study of intramolecular aggregations of solid-state structures arising from RAHB.

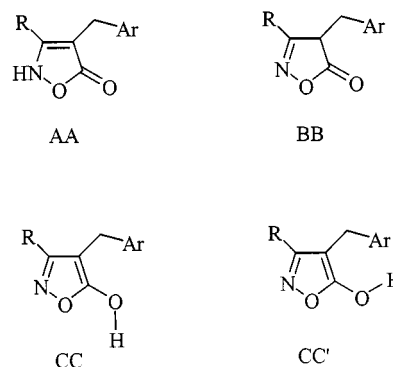


Figure 1. 4-(Arylmethyl)isoxazol-5-one derivatives; existing forms in solution

This paper describes a new synthesis and a structural investigation of these interesting molecules, the predominant solid-state forms of which can often be oriented with an appropriate choice of crystallization solvent.^[7]

Results and Discussion

Synthesis

The starting materials used in this study were 4-(arylmethylene)isoxazol-5-ones **1**, which, because of their simplicity and low preparation costs, as well as the marked reactivities of their exocyclic double bonds, offer the best route to the desired 4-arylmethyl derivatives **3**. The substrates **1**, in addition to their activity as dipolarophiles, dienophiles, and Michael acceptors, also function well as dehydrogenating agents in the homogeneous phase oxidation of benzimidazole to benzimidazole, thanks to the presence of the activated exocyclic double bond and are efficiently reduced to

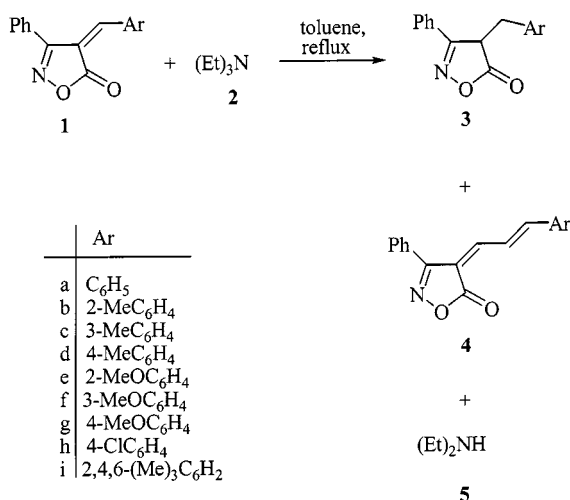
^[a] Dipartimento di Chimica Organica e Biologica, Università, Vill. S. Agata, 98166 Messina, Italy
Fax: (internat.) + 39-090/393-897
E-mail: ggrassi@isengard.unime.it

^[b] Dipartimento di Chimica Inorganica, Analitica e Struttura Molecolare, Università, Vill. S. Agata, 98166 Messina, Italy

Supporting information for this article is available on the WWW under <http://www.eurjoc.com> or from the author.

the corresponding arylmethylisoxazolones **3**.^[6] It thus seemed interesting to extend this reaction to other potential hydrogen donor systems such as triethylamine (TEA) and other suitable aliphatic tertiary amines. Indeed, in our reactions TEA, degrading to diethylamine (DEA), brought about not only the expected saturation of the exocyclic double bond in the arylmethylene derivative, but also a lengthening of its lateral chain.

Thus, we started out by heating **1** and **2** (in excess) with TEA in refluxing toluene and, after a careful workup, obtained arylmethylisoxazolones **3**, cinnamylidene derivatives **4**, and DEA (**5**) (Scheme 1). The yields of the products obtained are shown in Table 1.



Scheme 1

Table 1. Yields (%) of products **3** and **4**

Substrate	3	4
1a	75	23
1b	43	14
1c	45	12
1d	48	14
1e	20	18
1f	21	14
1g	32	16
1h	66	18
1i	40	12

All the 4-arylmethyl derivatives **3** were unequivocally identified by comparison with known authentic samples, while the structural assignment of 4-(cinnamylidene)isoxazolones **4** was based on analytical and spectroscopic data and confirmed by comparison of their IR and ¹H NMR spectra and those of analogous derivatives previously studied by one of us.^[8]

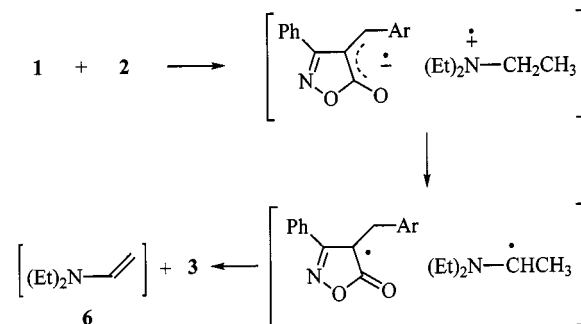
It is evident, therefore, that the isolation of DEA (**5**), which was characterised by gas chromatography, and the formation of cinnamylidene derivatives **4** through insertion of an ethylene unit into the exocyclic double bond of **1** clearly indicate the involvement of an ethyl group in the start-

ing TEA. To confirm this, the reaction was repeated with the substrate **1a** and other selected tertiary amines. As Table 2 indicates, the results obtained with amines containing ethyl groups (entries 1–3) were the same as those observed with TEA, while no reaction was observed with amines not containing ethyl groups (entries 4–6) and the starting material was recovered unchanged.

Table 2. Treatment of **1a** with tertiary amines

Entry	Amine	Products 3 and 4 recovered: overall yield [%]
1	<i>N,N</i> -Diethylaniline	95
2	<i>N,N</i> -Diisopropylethylamine	91
3	<i>N-tert</i> -Butyl- <i>N</i> -ethylisobutylamine	93
4	Trimethylamine	—
5	<i>N,N</i> -Diphenylmethylamine	—
6	Triphenylamine	—

It can therefore reasonably be hypothesized that our reaction proceeds through an initial dehydrogenation of TEA, as suggested in Scheme 2, analogously to the reaction between some aliphatic tertiary amines containing the CH–CH–N grouping and compounds that act as powerful electron acceptors.^[9]

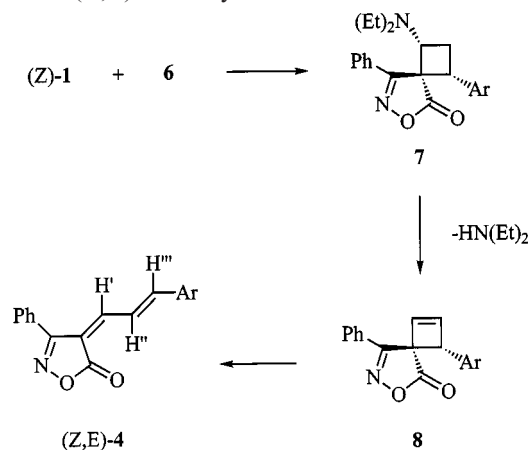


Scheme 2

In our case, the arylidene system favours the oxidation of the tertiary amine to enamine **6**. The proposed SET process, which is consistent with the reduction of 4-(arylidene)isoxazolones and pyrazolones derivatives with benzimidazolines generated in situ, is further confirmed by the observation that the benzyl product yields (Table 1) tend to decrease when groups with generally electron-releasing properties are introduced onto Ar. These groups are known to act by drastically reducing the electron-acceptor ability of electron-deficient olefins.

Furthermore, the fact that cinnamylidene derivatives **4** were obtained is conclusive proof of dehydrogenation of the tertiary starting amine occurring at the expense of the arylidene **1**. Indeed, if 4-arylidene isoxazolones and pyrazolones derivatives with benzimidazolines generated in situ, is further confirmed by the observation that the benzyl product yields (Table 1) tend to decrease when groups with generally electron-releasing properties are introduced onto Ar. These groups are known to act by drastically reducing the electron-acceptor ability of electron-deficient olefins.

In the light of the above observations and of our previous results, we postulate the pathway described in Scheme 3: formation of spiran **7** by a concerted [2+2] cycloaddition between (*Z*)-**1** and vinylamine **6**, followed by loss of DEA and thermal cycloreversion of the resulting cyclobutene **8** to give the (*Z,E*)-cinnamylidene derivative **4**.



Scheme 3

The discovery of this new synthesis pathway and the concrete hypothesis suggesting the considerable potential of arylmethyl **3** derivatives for use in practical applications prompted us to scrutinize certain properties of these intriguing molecules further. Our interest focussed in particular on the preparation of samples of **3** in the desired tautomeric form in the solid state; such samples are useful for study of their capacities for self-assembly into supramolecular systems through RAHB.

Thus, after a number of attempts, we selected derivatives **3e** and **3i**, obtained by crystallization from petroleum ether and methanol, respectively. On these two molecules and relative model systems representative of the tautomers of interest, we carried out structural characterization by X-ray analysis and *ab initio* and density functional calculations.

X-ray Crystal Structures of **3e** and **3i**

Figure 2 shows the structure of compound **3e** in its supramolecular aggregate and the atomic numbering scheme for the atoms and hydrogen bonds (represented by dotted lines). Selected bond lengths, angles, and some relevant torsion angles are given in Table 3, together with the corresponding values for compound **3i**.

Compound **3e** crystallises in the *P* $\bar{1}$ centrosymmetric space group, with six molecules in the elemental cell. The asymmetric unit is made up of three independent molecules [named A, B, and C] held together by strong hydrogen bonds in such a way as to form a rigid trimeric unit, described as a R $\bar{3}$ (15) graph set.^[10]

In the supramolecular aggregate, the arrangement of three molecules is comparable to the characteristic shape of a propeller rotor. The strong hydrogen bonds determine the formation of the trimeric supramolecular unit, which probably pre-exists in the liquid state and is so stable that it guides the entire process of crystal growth.

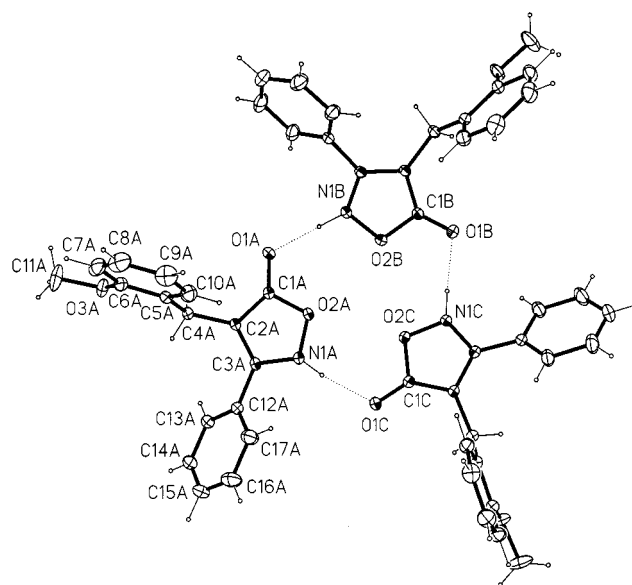


Figure 2. View of the asymmetric unit of compound **3e** (*AA*-type tautomer) with atom numbering scheme and thermal ellipsoids at 30% probability, while H size is arbitrary; dotted lines represent the H-interactions between the molecules in the trimeric unit (A, B and C, respectively)

The structural parameters of the three crystallographically independent molecules are, with few exceptions, equal within the e.s.d.s, and the arrangement of the trimer is such that it partly respects a non-crystallographic pseudosymmetrical ternary axis perpendicular to the median plane of the same trimeric unit.

The phenyl and the *p*-methoxybenzyl fragments are all oriented in the same direction, with the exception of the phenyl group of A, which is oriented in the opposite direction, thus destroying the ternary axis of symmetry.

Individually, the three central isoxazol-5-one rings are almost planar, but the central trimeric unit is somewhat folded, causing the entire aggregate to resemble a crystal glass without a stem.

The single molecules in the asymmetric unit are composed of an isoxazol-5-one ring bearing a phenyl and a *p*-methoxybenzyl group on the C(2)–C(3) double bond axis. As is obvious from the torsion angles of N(1)–C(3)–C(12)–C(17) [50.6(4), –52.5(4), and –41.4(4)° for the molecules A, B, and C, respectively], the three phenyl planes are significantly rotated with respect to the central pentatomic rings; some steric interactions are also responsible for the orientations of the *p*-methoxybenzyl groups.

The orientations of methoxyphenyl fragments with respect to the methylene hydrogen are such as to maximize C(4)⋯O(3) intramolecular interaction; moreover, just as with numerous other compounds^[11] containing one or two methoxy groups, the orientation of the group in relation to the aromatic ring is such as to favour extensive electronic delocalization from the oxygen O(3) lone-pairs to the phenyl. Such an interaction is possible when the methoxy group is coplanar with the ring; here, as can be seen from

Table 3. Comparison of selected geometric values for compounds **3e** and **3i** [Å, °]

	A	3e B	C	3i
C(1)–O(1)	1.229(2)	1.230(2)	1.233(2)	1.193(2)
C(1)–O(2)	1.385(2)	1.391(2)	1.391(2)	1.369(2)
C(1)–C(2)	1.410(2)	1.407(2)	1.412(2)	1.503(2)
C(2)–C(3)	1.368(2)	1.374(2)	1.372(2)	1.496(2)
C(2)–C(4)	1.492(2)	1.499(2)	1.501(2)	1.564(2)
C(3)–N(1)	1.339(2)	1.331(2)	1.332(2)	1.287(2)
C(3)–C(12)	1.478(2)	1.473(2)	1.474(2)	1.471(2)
N(1)–O(2)	1.395(2)	1.389(2)	1.390(2)	1.437(2)
C(4)–C(5)	1.518(2)	1.511(2)	1.508(2)	1.514(2)
C(6)–O(3)	1.368(2)	1.375(2)	1.369(2)	
O(3)–C(11)	1.435(2)	1.426(2)	1.436(2)	
O(1)–C(1)–O(2)	118.0(1)	117.3(1)	117.6(1)	120.4(2)
O(1)–C(1)–C(2)	133.7(1)	134.6(1)	134.5(1)	131.5(2)
O(2)–C(1)–C(2)	108.3(1)	108.1(1)	108.0(1)	108.1(1)
C(3)–C(2)–C(1)	106.4(1)	106.2(1)	106.2(1)	100.4(1)
C(3)–C(2)–C(4)	130.4(1)	128.3(1)	129.0(1)	116.5(1)
C(1)–C(2)–C(4)	123.2(1)	124.9(1)	124.2(1)	112.0(1)
N(1)–C(3)–C(2)	109.9(1)	109.9(1)	109.9(1)	113.4(1)
N(1)–C(3)–C(12)	119.2(1)	118.0(1)	118.1(1)	118.9(1)
C(2)–C(3)–C(12)	130.9(1)	132.1(1)	131.9(1)	127.7(1)
C(3)–N(1)–O(2)	109.3(1)	109.6(1)	109.6(1)	108.1(1)
C(1)–O(2)–N(1)	106.1(1)	106.1(1)	106.2(1)	109.9(1)
C(2)–C(4)–C(5)	116.2(1)	118.3(1)	118.1(1)	112.7(1)
C(6)–O(3)–C(11)	118.3(2)	118.0(1)	117.6(1)	
O(2)–C(1)–C(2)–C(3)	0.7(2)	1.4(2)	1.1(2)	–4.0(2)
O(1)–C(1)–C(2)–C(4)	0.2(3)	10.5(3)	8.6(3)	–58.9(2)
C(1)–C(2)–C(4)–C(5)	–77.8(2)	–82.0(2)	–88.2(2)	70.2(2)
C(2)–C(4)–C(5)–C(6)	176.9(1)	168.4(1)	176.1(1)	–104.1(2)
N(1)–C(3)–C(12)–C(17)	50.7(2)	–52.2(2)	–40.9(2)	7.5(2)
C(7)–C(6)–O(3)–C(11)	–5.9(3)	1.5(2)	–5.2(2)	
D–H...A	<i>d</i> (D–H)	<i>d</i> (H...A)	<i>d</i> (D...A)	(DHA)
N(1B)–H(1B)...O(1A)	0.95(2)	1.74(2)	2.697(2)	179(2)
N(1A)–H(1A)...O(1C)	0.90(2)	1.89(2)	2.782(2)	169(2)
N(1C)–H(1C)...O(1B)	0.92(2)	1.85(2)	2.769(2)	175(2)
C(17)–H(17)...N(1)	0.93	2.51	2.808(2)	98.7
C(18)–H(18B)...O(1)	0.96	2.58	3.305(2)	132.7

the mean value [176.1(2)°] of the torsion angles C(5)–C(6)–O(3)–C(11), it is. In order to favour the π -delocalization and to minimize steric interaction between the methyl group and the *ortho*-hydrogen atom, the C(5)–C(6)–O(3) and C(7)–C(6)–O(3) bond angles [114.9(1) and 123.9(1)°, respectively] are strongly distorted and this situation has been highlighted in numerous cases.^[12] Nevertheless, we are currently carrying out a crystallographic and ab initio study with the aim of interpreting this aspect thoroughly.

It is interesting to note that the structural parameters of the three independent molecules in the asymmetric unit are equal within the e.s.d.s, with the exception of the distances inside the pentatomic ring, where the few consistent variations are determined mainly by the slight differences in hydrogen bonds.

Bond lengths and angles indicate an extended electronic π -delocalization, which, thanks to the strongly RAHB-reinforced N–H...O bonds, involves the supramolecular system. This delocalization can occur by different 2³ pathways (LLL, SLL, LSL, LLS, LSS, SLS, SSL, SSS), since it can

take a long route L [O(1)–C(1)–C(2)–C(3)–N(1)] or a short one S [O(1)–C(1)–O(2)–N(1)] on each hetero ring. It cannot, however, be extended to the aryl rings, because of their relative orientations.

The structural values observed in the pentatomic ring are in excellent agreement with the corresponding values found in (*S*)-*N*-benzoyl-2-amino-3-(5-oxoisoxazolin-4-yl)propanoic acid^[13] [C(1)–C(2) 1.402(2), C(1)–O(2) 1.396(2), C(2)–C(3) 1.372(2), N(1)–C(3) 1.333(2), and N(1)–O(2) 1.384(2) Å]. The three C=O bond lengths [1.229(2), 1.230(2), and 1.233(2) Å for the molecules A, B, and C, respectively], although equal within the e.s.d.s, follow the course described above and, moreover, correspond to three N...O: 2.697(2), 2.769(2), and 2.782(2) Å for the Oa...Nb, Ob...Nc, and Oc...Na, respectively. The first of the three is, together with those seen in 2-arylpyrazolo[4,3-*c*]quinolin-3-ones,^[5a] one of the shortest N...O intermolecular separations observed to date and corresponds with the longest C=O distance. In our compound, both the N...O and the C=O distances are surprisingly shorter than any other set of reported values for analogous compounds in which π -de-

localization enhancement and RAHB are both operative.^[14]

The angles around the carbonyl carbon atoms [O(2)–C(1)–O(1), β ; C(2)–C(1)–O(1), α ; and O(2)–C(1)–C(2), γ] show significant asymmetry and have values of 118.0(2)°, 133.7(2)°, and 108.3(2)°, respectively. The pronounced difference in the exocyclic angles is determined^[15] both by steric and by electronic factors. It is consistently present in the more than 2800 compounds containing the O=C–O fragment [O=C=O, β ; X–C=O (X=C, N), α ; and O–C–X, γ] described in the CSD.^[16] The endocyclic γ angle, on the other hand, remains almost unchanged [mean value = 109.8(6)° over all compounds]. The $\Delta|\alpha - \beta|$ difference in exocyclic angles is also strongly influenced by the steric effects of the substituents in the 2-position but in all cases a significant difference is observed. We have found that, for compounds without steric strain, Δ is approximately 10°. Figure 3 shows the $\Delta|\alpha - \beta|$ difference versus α and β . When an sp^2 nitrogen atom (this means an O=C–N= fragment) is present on the pentatomic ring in the place of oxygen and its lone-pair is coplanar with the pentatomic ring, the asymmetry of the carbonyl carbon atom angles generally vanishes but in some cases the O=C–N (α) angle becomes larger than β .^[17] As we have already pointed out^[18] this asymmetry is observed consistently, but is, for example, a little less pronounced because of the slight strain in the coumarin esatomic ring.

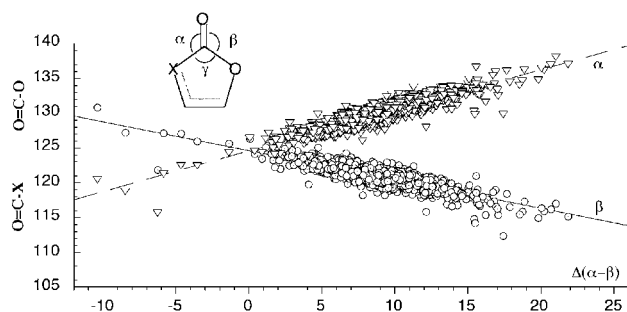


Figure 3. Scattergrams of the bond angles O=C–X (α) and O=C–O (β) vs. ($\alpha - \beta$) in CSD

Compound **3i**, shown in Figure 4, also presents the usual asymmetry in the bond angles to the carbonyl carbon: O(2)–C(1)–O(1) = 120.3(1); C(2)–C(1)–O(1) = 131.5(2), and O(2)–C(1)–C(2) = 108.1(1)°. Here, O(1) is involved in very weak intramolecular contact: O(1)⋯C(18) is 3.305(3) Å. The C(1)–O(1) bond length of 1.193(2) Å is significantly shorter than the corresponding distance found in **3e**, in which the strong hydrogen bond is responsible for C=O lengthening. The bond lengths and angles within the 4*H*-isoxazol-5-one are in good agreement with values so far reported for compounds containing this fragment.^[5a] In the molecular packing there is no significant hydrogen bond interaction, only normal van der Waals interaction and a graphite-like stacking interaction between the pentatomic ring and the phenyl group; this is in agreement with the

inability of the molecule to form RAHB, the stacking developing along the *b* axis as reported in Figure 5.

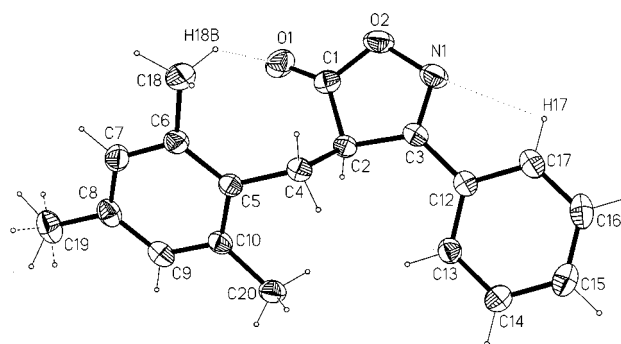


Figure 4. Molecule view of compound **3i** (BB-type tautomer) showing the atom numbering scheme, the intramolecular H bonds and the *p*-methyl rotational disorder (two staggered conformations with 0.5 occupancy); thermal ellipsoids are drawn at the 30% probability, while H size is arbitrary

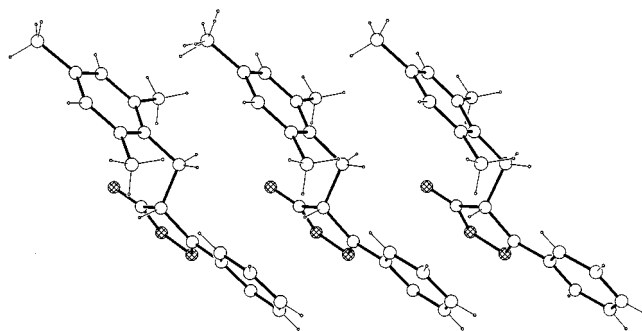


Figure 5. View of the overlapping of compound **3i** molecules translated along the crystallographic *b* axes (*x*, 1 + *y*, *z*) showing the strong π -stacking between the phenyl and isoxazolone rings of adjacent units; atom size is arbitrary and hydrogens are omitted for the sake of clarity

Ab initio and DFT Calculations

Ab initio and DFT calculations were performed on the AA tautomer model without substituents (see Figure 1) with the aim of establishing the relative stability of supramolecular complexes with respect to the monomer and to estimate the extent of π -delocalization and RAHB-induced stabilization. Single-point (SP) energy calculations performed at several levels of complexity on the monomer and trimer models show how the strong hydrogen bonds promote a more pronounced degree of stabilization (40 ± 1 kcal/mol) in the cyclic trimer than in the monomer at a high level of calculation [HF/6-311++G(d,p), MP2/6-31++G(d,p), B3LYP/6-31++G(d,p)]. The linear dimer and trimer, for which SP energies were calculated only at the B3LYP/6-31+G(d) level, are more stable than the monomer (at 10.8 and 21.8 kcal/mol, respectively). The bond length and angles in the optimized geometry of the trimeric model are in good agreement with the values derived from X-ray analysis; full details of our analyses will be published elsewhere.

In order to investigate the relative stabilities of the four forms in **3e** in the gas phase, further ab initio and DFT

Table 4. Ab initio and DFT SP energy (Hartree) calculations on 2*H*-isoxazol-5-one tautomers

Method	AA	CC'	CC	BB	$\Delta E^{[a]}$	$\Delta E^{[b]}$
HF/STO-3G	-315.28693	-315.31920	-315.32267	-315.33844	2.2	32.3
HF/3-21G*	-317.65230	-317.64577	-317.65164	-317.66602	3.7	12.7
HF/6-31G	-319.28872	-319.27991	-319.28615	-319.29447	3.9	9.1
HF/6-311+G	-319.37727	-319.37025	-319.37592	-319.38315	3.6	8.1
HF/6-31G(d)	-319.44479	-319.44784	-319.45123	-319.46505	2.1	12.7
HF/6-31+G(d,p)	-319.46368	-319.46777	-319.47110	-319.47844	2.1	9.3
HF/6-31++G(d,p)	-319.46380	-319.46790	-319.47125	-319.47856	2.1	9.3
HF/6-311++G(d,p)	-319.53471	-319.53843	-319.54170	-319.54789	2.1	8.3
MP2/6-311++G(d,p)	-319.53472	-319.53845	-319.54172	-319.54796	2.1	8.3
B3LYP/6-31G(d)	-321.24740	-321.24536	-321.24865	-321.26493	2.1	11.0
B3LYP/6-31+G(d)	-321.26432	-321.26052	-321.26392	-321.27925	2.1	9.4
B3LYP/6-311++G(d,p)	-321.34908	-321.34679	-321.35016	-321.35945	2.1	6.5

^[a] $\Delta[ECC' - ECC]$ (kcal/mol). ^[b] $\Delta[EBB - EAA]$ (kcal/mol).

calculations were also performed on model fragments of AA, BB, CC and CC' (Figure 1). Calculations performed at several levels of complexity by either method indicated the following stability order: $CC \approx AA < CC' < BB$ (in agreement with the previous results).^[7] BB is the lowest energy tautomer, the energy gap between tautomers BB and AA is ca. 9 kcal/mol, while the energy gap between the two conformers CC and CC' is ca. 2.1 kcal/mol. The CC' conformer is the more stable of the latter pair, thanks to the formation of the intramolecular hydrogen bond present in this conformation. Table 4 shows energy values calculated by using the two methods and the various basic sets, together with relative differences (in kcal/mol) between the most and the least stable tautomers, together with values for CC and CC'. Table 4 also shows that DFT (B3LYP functional) overestimates the energy gap only between the AA and the CC tautomers. With B3LYP at 6-31+G(d) level, we also estimated (4.8 kcal/mol) the torsional barrier (Figure 6) for the enol tautomers, by scanning the torsion angle of the enol group at 20° intervals between 0° (CC' conformer) and 180° (CC conformer).

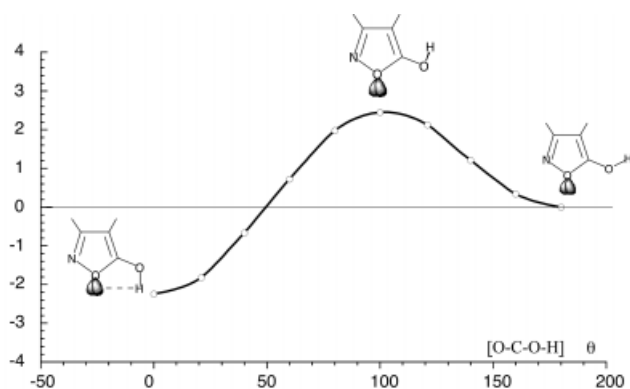


Figure 6. Variation of the torsional energy in the tautomer C computed at B3LYP/6-31+G(d) level

Conclusions

In conclusion, we have described in this paper a simple and mild procedure for the preparation of 4-arylmethylisoxazol-5-ones from the corresponding arylmethylene derivatives by use of selected tertiary amines as reductive agent. Our results have also demonstrated that the solid-state 4*H*-isoxazol-5-one system, in the tautomeric form necessary to allow self-assembly through RAHB and thus incorporated in more complex structures, might represent central building units for as yet unexplored supramolecular architectures.

Experimental Section

General: Melting points were determined on Reichert–Kofler hot-stage microscope and are uncorrected. Elemental analyses were performed on Carlo Erba EA 1102 machine. Infrared spectra were obtained as KBr pellets on a Nicolet FT-IR Impact 400D spectrometer. ¹H NMR spectra were recorded with a Bruker ARX 300 instrument. Column chromatography was performed on Merck silica gel 70–270 mesh. – All solvents and reagents were obtained from commercial sources and purified before use if necessary. 4-(Arylmethylene)isoxazol-5-ones **1** were prepared by standard procedures.

General Procedure for Treatment of the 4-(Arylmethylene)isoxazol-5-ones **1 with TEA:** Arylmethylisoxazolones **1** (10 mmol) and TEA (15 mmol) were dissolved in toluene (80 mL) and the mixture was refluxed for 2 hours. After cooling, the mixture was extracted twice with 40 mL of an aqueous saturated Na₂CO₃ solution and the two layers were separated:

(a) The dark violet basic aqueous layer was then acidified with a 10% aqueous solution of HCl and extracted with ether. The organic layer was dried with MgSO₄ and, after filtration, evaporated under reduced pressure. The residue was purified by crystallization (petroleum ether) to yield arylmethylisoxazolones **3** (Table 1) as colourless needles.

Table 5. Summary of crystal data and structure refinement for compounds **3e** and **3i**

	3e	3i
Empirical formula	C ₁₇ H ₁₅ NO ₃	C ₁₉ H ₁₉ NO ₂
Molecular mass	281.30	293.35
Crystal system, space group	Triclinic, <i>P</i> $\bar{1}$	Monoclinic, <i>P</i> ₂ <i>1</i> / <i>c</i>
Unit cell dimensions		
<i>a</i> [Å]	11.989(2)	20.033(2)
<i>b</i> [Å]	14.160(2)	5.1877(5)
<i>c</i> [Å]	15.295(2)	14.669(2)
α [°]	107.44(1)	90
β [°]	106.54(1)	92.646(8)
γ [°]	107.47(1)	90
Volume [Å ³]	2153.4(5)	2087.4(5)
<i>Z</i>	6	4
Density (calculated) [Mg/m ³]	1.301	1.279
Absorption coefficient [mm ⁻¹]	0.090	0.083
<i>F</i> (000)	888	624
Crystal size [mm ³]	0.60 × 0.35 × 0.30	0.80 × 0.42 × 0.25
Data collection theta range [°]	2.42–25.05	2.04–25.00
Scan type	ω – 2 θ	ω
Reflections collected	8259	3718
Independent reflections	7643 [<i>R</i> (int) = 0.0087]	2683 [<i>R</i> (int) = 0.0199]
Absorption correction	ϕ -scan (<i>t</i> = 0.9736/0.9481)	none
Data/restraints/parameters	7643/0/581	2683/0/200
Goodness-of-fit on <i>F</i> ²	0.838	0.955
Final <i>R</i> indices [<i>I</i> > 2 σ (<i>I</i>)]	<i>R</i> 1 = 0.0340, <i>wR</i> 2 = 0.0761	<i>R</i> 1 = 0.0390, <i>wR</i> 2 = 0.1016
<i>R</i> indices (all data)	<i>R</i> 1 = 0.0591, <i>wR</i> 2 = 0.0807	<i>R</i> 1 = 0.0526, <i>wR</i> 2 = 0.1130
Extinction coefficient	0.0089(6)	0.009(2)
Largest diff. peak and hole [e·Å ⁻³]	0.161 and –0.134	0.147 and –0.143

(b) The organic phase was dried (MgSO₄), filtered, and concentrated to dryness. The residue was purified by column chromatography (chloroform) to provide **4** (Table 1) as an orange solid.

The IR and ¹H NMR spectra were identical to and superimposable on those of **3**^[6] and **4**,^[8] reported previously.

Crystallographic Data: A short summary of X-ray structure determination data for the two compounds **3e** and **3i** is reported in Table 5. A comparison of the significant geometric values of the three single isoxazolones constituting the trimer **3e** and of the molecule of **3i** is given in Table 3. Both colourless crystal samples suitable for X-ray analysis were obtained by crystallization from petroleum ether and methanol, respectively. Diffraction data for both compounds were collected at room temperature with a Siemens P4 automated four-circle, single-crystal diffractometer and graphite-monochromated Mo-*K*_α radiation (λ = 0.71073 Å). Lattice parameters were obtained from least-squares refinement of the setting angles of 35 and 29 reflections and were $23 \leq 2\theta \leq 27^\circ$ and $10 \leq 2\theta \leq 25^\circ$ respectively. Diffraction data were processed by the learnt-profile procedure^[19] and then corrected for Lorentz polarization effects. Standard deviations $\sigma(I)$ were estimated from counting statistics. Absorption correction was applied to **3e** data only, by fitting a pseudo-ellipsoid to the azimuthal scan data of 20 suitable reflections with high χ angles.^[20] The statistics $|E^2 - 1|$ and consistent absences for compound **3i** pointed to the centrosymmetric space groups *P* $\bar{1}$ and *P*₂*1*/*c* respectively. Data collection and reduction was performed by the SHELXTL^[21] package for **3e** and XSCANS^[22] for **3i**.

Both structures were solved by a combination of standard Direct Methods^[23] and Fourier synthesis, and refined by minimization of the $\Sigma w(F_o^2 - F_c^2)^2$ function with a full-matrix, least-squares technique based on all independent *F*² data and all anisotropic non-

hydrogen atoms using SHELXL97.^[24] For **3i**, hydrogen atoms were included in both the refinements by use of the “riding model” method, with X–H bond geometry and the isotropic displacement parameter depending on the parent atom. In model **3e**, the three nitrogen hydrogens were located on the Fourier difference map and refined isotropically without constraint. In model **3i**, rotational disorder was taken into account for the less hindered *p*-methyl group of the phenyl substituent.

An empirical extinction parameter was included in the final refinement cycles of both models. Neither of the last difference Fourier maps showed any significant electron density residuals.

Final geometrical calculations and drawings were carried out with the PARST program^[25] and the XP utility,^[26] respectively. Crystallographic data (excluding structure factors) for the structures reported in this paper have been deposited with the Cambridge Crystallographic Data Centre as supplementary publication nos. CCDC–165933 and –165934 for compound **3e** and **3i**, respectively. Copies of the data can be obtained free of charge on application to CCDC, 12 Union Road, Cambridge CB2 1EZ, UK [Fax: (internat.) + 44-1223/336-033; E-mail: deposit@ccdc.cam.ac.uk].

Computational Details

Ab initio and DFT calculations, molecular modelling and geometry optimization were carried out with the Gaussian98^[27] series of programs. Ab initio geometry optimization on tautomers AA, BB, and CC, as well as on the trimeric complex of tautomer AA, was performed at HF/6-31+G(d,p) level.

Single-point (SP) energy calculations for all tautomers, conformer CC' and the supramolecular complex of tautomer AA were performed at several levels of complexity, starting with HF/STO-3G and ending with the more sophisticated B3LYP/6-31++G(d,p). A

complete list of the basic sets used is reported in Table 4. The torsional barrier of the CC' tautomers was computed by B3LYP at 6-31+G(d) level, by scanning the torsional angle of the enol group (O–C–O–H) at 20° intervals between 0° (CC' conformer) and 180° (CC conformer).

- [1] P. Dauber, A. Hagler, *Acc. Chem. Res.* **1980**, *13*, 105–112.
- [2] J. A. Sussman, *Mol. Cryst. Liq. Cryst.* **1972**, *18*, 39–51.
- [3] D. Y. Curtin, I. C. Paul, *Chem. Rev.* **1981**, *81*, 525–541.
- [4] G. Gilli, F. Bellucci, V. Ferretti, V. Bertolasi, *J. Am. Chem. Soc.* **1989**, *111*, 1023–1028.
- [5] [5a] V. Bertolasi, P. Gilli, V. Ferretti, G. Gilli, *Acta Crystallogr., Sect. B* **1995**, *51*, 1004–1005. [5b] G. Gilli, P. Gilli, *J. Mol. Struct.* **2000**, *552*, 1–16.
- [6] F. Risitano, G. Grassi, F. Caruso, F. Foti, *Tetrahedron* **1996**, *52*, 1443–1450.
- [7] C. J. Cramer, D. G. Truhlar, *J. Am. Chem. Soc.* **1993**, *115*, 8810–8817.
- [8] A. Maquestiau, Y. Van Haverbeke, R. N. Muller, G. Lo Vecchio, G. Grassi, *Tetrahedron Lett.* **1973**, 4249–4251.
- [9] D. Buckley, S. Dunstan, H. B. Henbest, *J. Chem. Soc.* **1957**, 4880–4891.
- [10] J. Bernstein, R. E. Davis, L. Shimoni, N. L. Chang, *Angew. Chem. Int. Ed. Engl.* **1995**, *34*, 1555–1573.
- [11] [11a] G. Salem, A. Terzis, D. Mentzafos, *Acta Crystallogr., Sect. C* **1988**, *44*, 385–386. [11b] F. Viladomat, J. Bastida, C. Codina, X. Solans, M. Font-Bardia, *Acta Crystallogr., Sect. C* **1999**, *55*, 385–387. [11c] N. K. Sharma, R. Kumar, V. S. Parmar, W. Errington, *Acta Crystallogr., Sect. C* **1997**, *53*, 1438–1440. [11d] R. Kumar, V. S. Parmar, W. Errington, J. Wengel, C. E. Olsen, *Acta Crystallogr., Sect. C* **1998**, *54*, 363–365. [11e] A. Elmali, M. Kabak, Y. Elerman, *J. Mol. Struct.* **1999**, *484*, 229–234. [11f] Yung-Sing Wong, C. Marazano, D. Gnecco, Y. Genisson, A. Chiaroni, B. C. Das, *J. Org. Chem.* **1997**, *62*, 729–732. [11g] M. O. Abdellahi, T. Jouini, *Acta Crystallogr., Sect. C* **1995**, *51*, 924–926.
- [12] [12a] H. Bock, A. Rauschenbach, C. Nather, Z. Havlas, A. Gavezotti, G. Filippini, *Angew. Chem. Int. Ed. Engl.* **1995**, *34*, 76–78. [12b] W. Hummel, K. Huml, H.-B. Burgi, *Helv. Chim. Acta* **1988**, *71*, 1291–1303.
- [13] S. Tsubotani, Y. Funabashi, M. Takamoto, S. Hokoda, S. Harada, *Tetrahedron* **1991**, *47*, 8079–8090.
- [14] V. Ferretti, V. Bertolasi, G. Gilli, P. A. Borea, *Acta Crystallogr., Sect. C* **1985**, *41*, 107–110.
- [15] [15a] F. Risitano, G. Grassi, G. Bruno, F. Nicolò, *Liebigs Ann./Recueil* **1997**, 441–445. [15b] G. Bruno, F. Nicolò, A. Rotondo, G. Grassi, F. Foti, F. Risitano, C. Bilardo, *Acta Crystallogr., Sect. E* **2001**, *57*, o396–o398. [15c] G. Bruno, F. Nicolò, A. Rotondo, G. Grassi, F. Foti, F. Risitano, C. Bilardo, *Acta Crystallogr., Sect. E* **2001**, *57*, o399–o401. [15d] G. Bruno, G. Grassi, F. Risitano, F. Foti, F. Nicolò, *Heterocycles* **2001**, 763–768.
- [16] F. H. Allen, J. E. Davies, J. J. Galloy, O. Johnson, O. Kennard, C. F. Macrae, E. M. Mitchell, G. F. Mitchell, J. M. Smith, D. G. Watson, *J. Chem. Info. Comp. Sci.* **1991**, *31*, 187–194.
- [17] [17a] P. Gluzinski, J. Rajewski, J. Lange, G. D. Andretti, G. Bocelli, *Acta Crystallogr., Sect. C* **1984**, *40*, 108–110. [17b] R. Prevo, J. H. Bieri, U. Vvidmer, H. Heimgartner, *Helv. Chim. Acta* **1981**, 1515–1521.
- [18] G. Bruno, F. Nicolò, A. Rotondo, G. Grassi, F. Foti, F. Risitano, C. Bilardo, *Acta Crystallogr., Sect. C* **2001**, *57*, 493–494.
- [19] A. Quilico, *The Chemistry of Heterocyclic Compounds*, in the Wiley R. H., Wiley-Interscience, New York, **1962**, 117, and references therein.
- [20] R. Diamond, *Acta Crystallogr., Sect. A* **1969**, *25*, 43–55.
- [21] G. Kopfmann, R. Huber, *Acta Crystallogr., Sect. A* **1968**, *24*, 348–351.
- [22] *Siemens P3/V and SHELXTL-PLUS*, Vax-VMS version 4.21, Siemens Analytical X-ray Instruments Inc., Madison Wisconsin, **1991**.
- [23] Bruker. *XSCANS, release 2.31*, Bruker AXS Inc., Madison Wisconsin, **1999**.
- [24] A. Altomare, O. Cascarano, C. Giacovazzo, A. Guagliardi, M. C. Burla, G. Polidori, M. Camalli, *J. Appl. Cryst.* **1994**, *27*, 435–436.
- [25] G. M. Sheldrick, *SHELXL97. Program for Crystal Structure Refinement*. Univ. of Göttingen, Germany, **1997**.
- [26] M. Nardelli, *J. Appl. Chem.* **1995**, *28*, 659, version locally modified.
- [27] G. M. Sheldrick, *SHELXTL, VMS version 5.05*, Siemens Analytical X-ray Instruments Inc., Madison Wisconsin, **1991**.
- [28] M. J. Frisch, G. W. Trucks, H. B. Schlegel, G. E. Scuseria, M. A. Robb, J. R. Cheeseman, V. G. Zakrzewski, J. A. Montgomery, Jr., R. E. Stratmann, J. C. Burant, S. Dapprich, J. M. Millam, A. D. Daniels, K. N. Kudin, M. C. Strain, O. Farkas, J. Tomasi, V. Barone, M. Cossi, R. Cammi, B. Mennucci, C. Pomelli, C. Adamo, S. Clifford, J. Ochterski, G. A. Petersson, P. Y. Ayala, Q. Cui, K. Morokuma, D. K. Malick, A. D. Rabuck, K. Raghavachari, J. B. Foresman, J. Cioslowski, J. V. Ortiz, A. G. Baboul, B. B. Stefanov, G. Liu, A. Liashenko, P. Piskorz, I. Komaromi, R. Gomperts, R. L. Martin, D. J. Fox, T. Keith, M. A. Al-Laham, C. Y. Peng, A. Nanayakkara, M. Challacombe, P. M. W. Gill, B. Johnson, W. Chen, M. W. Wong, J. L. Andres, C. Gonzalez, M. Head-Gordon, E. S. Replogle, J. A. Pople. *Gaussian 98, Revision A.9*, Gaussian, Inc., Pittsburgh PA, **1998**.

Received July 4, 2001
[O01326]